



## Preparation and Characterization of Magnetic $\text{Co}_{0.5}\text{Mn}_{0.5}\text{Fe}_2\text{O}_4$ -Chitosan Nanoparticles as Surfactants in Oilfield

X.F. ZHENG and Q. LIAN\*

College of Chemical Engineering, Hebei Normal University of Science and Technology, Qinhuangdao 066600, P.R. China

\*Corresponding author: Tel: +86 24 2027029; E-mail: xuefang-zheng@163.com

Received: 25 February 2014;

Accepted: 25 April 2014;

Published online: 5 July 2014;

AJC-15505

The novel magnetic  $\text{Co}_{0.5}\text{Mn}_{0.5}\text{Fe}_2\text{O}_4$ -chitosan nanoparticles has the advantage of excellent biodegradation and a high level of controllability. The  $\text{Co}_{0.5}\text{Mn}_{0.5}\text{Fe}_2\text{O}_4$ -chitosan nanoparticles was prepared successfully. The size of the  $\text{Co}_{0.5}\text{Mn}_{0.5}\text{Fe}_2\text{O}_4$ -chitosan nanoparticles were all below 100 nm. The saturated magnetization of the  $\text{Co}_{0.5}\text{Mn}_{0.5}\text{Fe}_2\text{O}_4$ -chitosan nanoparticles could reach 80 emu/g and showed the characteristics of super-paramagnetism at the same time. The images of TEM and SEM electron microscopy showed that the cubic-shape magnetic  $\text{Co}_{0.5}\text{Mn}_{0.5}\text{Fe}_2\text{O}_4$  particles were encapsulated by the spherical chitosan nanoparticles. The evaluation on the interfacial properties of the product showed that the interfacial tension between crude oil and water could be reduce to ultra-low values as low as  $10^{-3}$  mN/m when the magnetic  $\text{Co}_{0.5}\text{Mn}_{0.5}\text{Fe}_2\text{O}_4$ -chitosan nanoparticle was used in several blocks in Shengli oilfield without other additives. Meanwhile, the magnetic  $\text{Co}_{0.5}\text{Mn}_{0.5}\text{Fe}_2\text{O}_4$ -chitosan nanoparticles possessed good salt-resisting capacity.

**Keywords:** Magnetic nanoparticles, Surfactants, Superparamagnetism, Interfacial tension.

### INTRODUCTION

Chitosan is the alkaline deacetylated product of chitin which is derived from the exoskeleton of crustaceans. It is hydrophilic, biocompatible, non-toxic, biodegradable. Due to the presence of both hydroxyl and amine groups in its structure, chitosan can be chemically modified to be used as novel separation media<sup>1-3</sup>. So, chitosan and its derivative have been widely used in the field of medicine, pharmacy and biotechnology. Chang and co-workers had prepared carboxymethylated magnetic particles by carboxymethylated the chitosan and bound onto  $\text{Fe}_3\text{O}_4$  nanoparticles *via* carbodiimide activation. The carboxymethylated chitosan-conjugated  $\text{Fe}_3\text{O}_4$  nanoparticles were shown to be quite efficient as anionic magnetic nano-adsorbent for the removal of acid dyes and heavy metal ions<sup>4-6</sup>.

Surface-active agents or surfactants are an important class of chemical compounds used in different sectors of modern industry, such as food, pharmaceutical, cosmetics and petroleum industries<sup>7,8</sup>. These compounds are able to reduce surface and interfacial tensions, as well as to form and stabilize oil in water (o/w) or water in oil (w/o) emulsions especially in adsorption of oil for enhanced oil recovery<sup>9</sup>. Currently, the alkyl benzene sulfonate<sup>10</sup> is widely used in enhanced oil recovery which has serious pollution<sup>11</sup>, difficulty to recycling<sup>12</sup> and non-

directional movement ability. Due to environmental issues and artificial surfactant, the demand for biodegradable surfactants and controlling direction of the microemulsion with surfactants is increasing.

Super-paramagnetic iron oxide nanoparticles have attracted researchers in various fields such as physics<sup>13</sup>, medicine<sup>14</sup>, biology<sup>15-17</sup> and materials science<sup>18,19</sup> due to their multifunctional properties such as small size, super-paramagnetism and low toxicity. However, the nanoparticles tend to aggregate due to strong magnetic dipole-dipole attractions between particles between particles. At the same time, the capacity for anti-acid, anti-alkali and anti-salt of magnetic nanoparticles is in the low level. Recently, the combination of organic and inorganic components at nano-sized level has attracted considerable attention because of the potential applications in many field<sup>20-23</sup>.

In this paper, magnetic  $\text{Co}_{0.5}\text{Mn}_{0.5}\text{Fe}_2\text{O}_4$ -chitosan nanoparticles were obtained using  $\text{Co}_{0.5}\text{Mn}_{0.5}\text{Fe}_2\text{O}_4$  as cores and chitosan as a polymeric shell. The size, structure and magnetic properties of the resultant magnetic nanoparticles were characterized by TEM, SEM, XRD and vibrating sample magnetometer. The binding of chitosan to the magnetic nanoparticles was confirmed by Fourier transform infrared (FT-IR) spectroscopy. The performance of surface-active was measured by TX-500C full-scale automatic dynamic spinning drop interfacial tension instrument.

## EXPERIMENTAL

Chitosan ( $M_w = 1 \times 10^5$ , deacetylating degree 95.5 %) were purchased from YuHuan Chemical Company, Zhejiang Province, China Glutaraldehyde solution (50 %), span-80, liquid paraffin, petroleum ether, ethanol, glacial acetic acid, sodium hydroxide, acetone,  $\text{Co}_{0.5}\text{Mn}_{0.5}\text{Fe}_2\text{O}_4$  (homemade).

**Preparation of magnetic chitosan nanoparticles:** According to mass ratio of  $\text{Co}_{0.5}\text{Mn}_{0.5}\text{Fe}_2\text{O}_4$  and chitosan is 1:4, 0.5 g  $\text{Co}_{0.5}\text{Mn}_{0.5}\text{Fe}_2\text{O}_4$  magnetic particles was quickly added into the 40 mL acetic acid solution (5 % v/v) which contained 2 g chitosan. The solution was placed in the ultrasonic reactor for 10 min. At the same time, control the frequency of ultrasonic is 22 KHz and the power is 1000 w to disperse the chitosan and the magnetic particles uniformly. After that, add 40 mL liquid paraffin and 10 drops of span-80. Then the solution is placed in the ultrasonic reactor for 0.5 h. In this work, the ultrasonic frequency is 22 KHz and the power is 500 w. To active  $\text{Co}_{0.5}\text{Mn}_{0.5}\text{Fe}_2\text{O}_4$  to get better magnetic properties, the reaction systems were kept at 60 °C for 5 h in a water bath. The cross-linked magnetic chitosan nanoparticles were formed by adding 2 mL of glutaraldehyde and by keeping the same condition for 5 h. After reaction, the prepared nanoparticles was precipitated with centrifugation (8000 rpm for 1 h) and rinsed with ethanol and deioned water for four times. Finally, the prepared nanoparticles were freeze dried for 24 h.

**Characterizations of magnetic chitosan nanoparticles:** X-ray power diffraction (XRD) measurement was performed using a Bruker D8 diffractometer with monochromatized  $\text{CuK}\alpha$  radiation ( $\lambda = 1.5426 \text{ \AA}$ ), 40 kV, 30 mA. Fourier transform infrared spectroscopy (FTIR, IRP restige-21, Shimadzu Inc.) was used to conform the structure of the magnetic  $\text{Co}_{0.5}\text{Mn}_{0.5}\text{Fe}_2\text{O}_4$ -chitosan nanoparticles. The magnetic chitosan nanoparticles were observed by transmission electron microscope (TEM, H-7650, Hitachi Inc.) to confirm the size and morphology. The sample of  $\text{Co}_{0.5}\text{Mn}_{0.5}\text{Fe}_2\text{O}_4$ -chitosan nanoparticles for TEM analysis was obtained by placing a drop of the nanoparticle dispersed ethyl solution onto a copper micro-grid and evaporated in 20 °C. The surface of the magnetic particles is detected by the scanning electron microscope (SEM, Kyky-2800, Kyky technology Co., Ltd). The elemental analysis of the particles was analyzed by elemental analyzer (Vario EL III, Elementar Inc.). Magnetic measurement were done in a vibrating sample magnetometer (VSM, PPMS-9, Quantum Design). The sample power was placed in a Teflon-coated sample holder and the mass was accurately measured.

**Determination of surface activity of the products:** The  $\text{Co}_{0.5}\text{Mn}_{0.5}\text{Fe}_2\text{O}_4$ -chitosan nanoparticles were mixed with 100 mL injected water corresponding to the oil block. Put a drop crude oil (about 0.1 mL) into the mixture and determine the oil-water interfacial tension.

The performance of surface-active depends on the activity to oil-water interface of the products. We use TX-500C full-scale automatic dynamic spinning drop interfacial tension instrument to measure the crude oil in GD-3, GD-4, GD-6, GD-7 oil block from Shengli oilfield in China after dehydrated and degassed. When injected water interfacial tension changed corresponding to time, the products should be able to reduce the oil-water interfacial tension to  $10^{-3}$  mN/m and below without

any other additives. Unless otherwise specified, the surface-active and anti-salt performance was tested in GD-3 from Shengli Oilfield in China after dehydrated and degassed corresponding to injected water. Furthermore, the products accounted for 0.4 % of the injected water.

## RESULTS AND DISCUSSION

**FTIR:** The curves a, b and c in Fig. 1 were the Infrared Spectroscopy of  $\text{Co}_{0.5}\text{Mn}_{0.5}\text{Fe}_2\text{O}_4$ -chitosan nanoparticles, chitosan particles and the  $\text{Co}_{0.5}\text{Mn}_{0.5}\text{Fe}_2\text{O}_4$  particles. As can be seen from the curve a, there was a new absorption peak at  $1635 \text{ cm}^{-1}$  that was peak of Schiff base absorption peak. That indicated that the glutaraldehyde indeed involved in the cross-linking reaction. The peak at  $580.5 \text{ cm}^{-1}$  was a characteristic absorption peak of the magnetic  $\text{Co}_{0.5}\text{Mn}_{0.5}\text{Fe}_2\text{O}_4$  particles showed that  $\text{Co}_{0.5}\text{Mn}_{0.5}\text{Fe}_2\text{O}_4$  magnetic particles effectively crosslinked chitosan particles. In the curve b, between  $3400\text{--}3200 \text{ cm}^{-1}$  peaks were caused by stretching vibration of the -OH in chitosan and hydrogen bonding, between  $3500\text{--}3400 \text{ cm}^{-1}$  peaks were caused by the N-H bond stretching vibration, the absorption peak near  $2900 \text{ cm}^{-1}$  was caused by C-H bond stretching vibration, the absorption peak in  $1617 \text{ cm}^{-1}$  was caused by amide bond in chitosan,  $1375 \text{ cm}^{-1}$  was  $\text{CH}_3$  and  $\text{CH}_2$  absorption peaks. Curve c was an infrared spectrum of the  $\text{Co}_{0.5}\text{Mn}_{0.5}\text{Fe}_2\text{O}_4$  particles. Contrasting curves a, b and c showed that the curve c contained all the characteristic peaks of the curve a and b,  $\text{Co}_{0.5}\text{Mn}_{0.5}\text{Fe}_2\text{O}_4$  magnetic particles were wrapped by chitosan particles successfully.

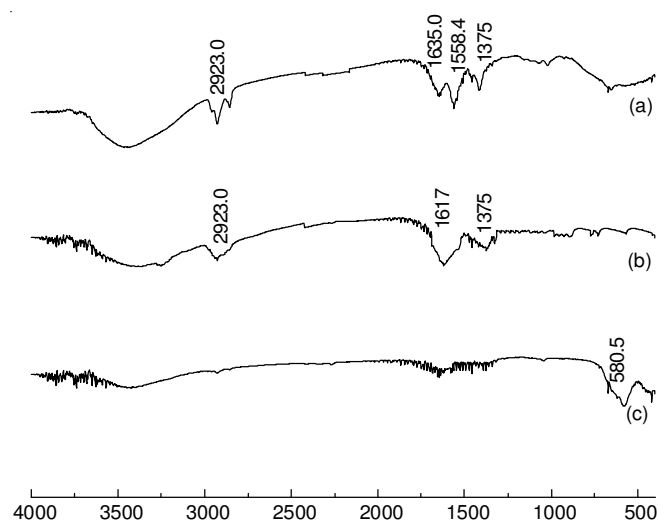


Fig. 1. FTIR spectra of samples: (a)  $\text{Co}_{0.5}\text{Mn}_{0.5}\text{Fe}_2\text{O}_4$ -chitosan nanoparticles, (b) chitosan nanoparticles, (c)  $\text{Co}_{0.5}\text{Mn}_{0.5}\text{Fe}_2\text{O}_4$  particles

**XRD:** All the diffraction peaks in Fig. 2 confirmed the component of the  $\text{Co}_{0.5}\text{Mn}_{0.5}\text{Fe}_2\text{O}_4$ -chitosan nanoparticles. The XRD result of the magnetic chitosan particles and pure  $\text{Co}_{0.5}\text{Mn}_{0.5}\text{Fe}_2\text{O}_4$  particles were mostly coincident. The magnetic chitosan particles were validated as the binding of chitosan and  $\text{Co}_{0.5}\text{Mn}_{0.5}\text{Fe}_2\text{O}_4$ .

**TEM:** The TEM images of  $\text{Co}_{0.5}\text{Mn}_{0.5}\text{Fe}_2\text{O}_4$  particles (Fig. 3) and  $\text{Co}_{0.5}\text{Mn}_{0.5}\text{Fe}_2\text{O}_4$ -chitosan nanoparticles particles (Fig. 4) showed the average diameter of the particles. The size of the  $\text{Co}_{0.5}\text{Mn}_{0.5}\text{Fe}_2\text{O}_4$  particles was varied from 30 to 10 nm.

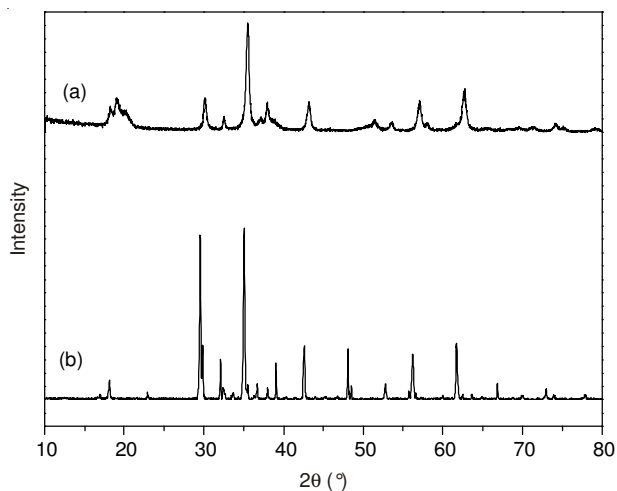


Fig. 2. XRD of cross-link magnetic chitosan nanoparticles (a) and  $\text{Co}_{0.5}\text{Mn}_{0.5}\text{Fe}_2\text{O}_4$  particles (b)

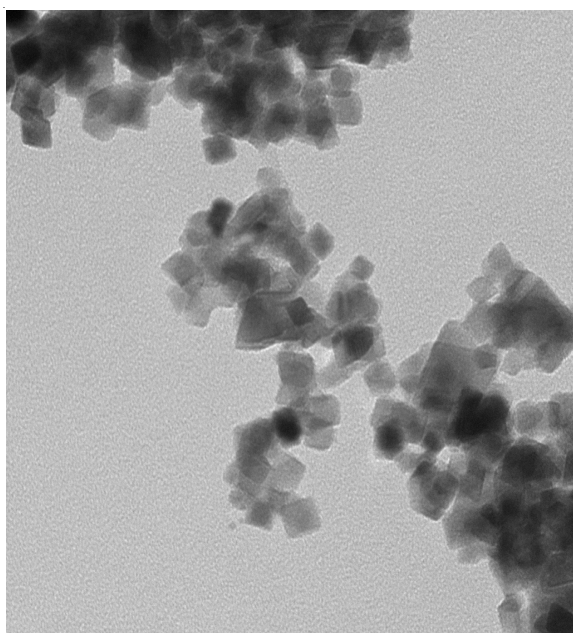


Fig. 3. TEM micrographs for the  $\text{Co}_{0.5}\text{Mn}_{0.5}\text{Fe}_2\text{O}_4$  particles

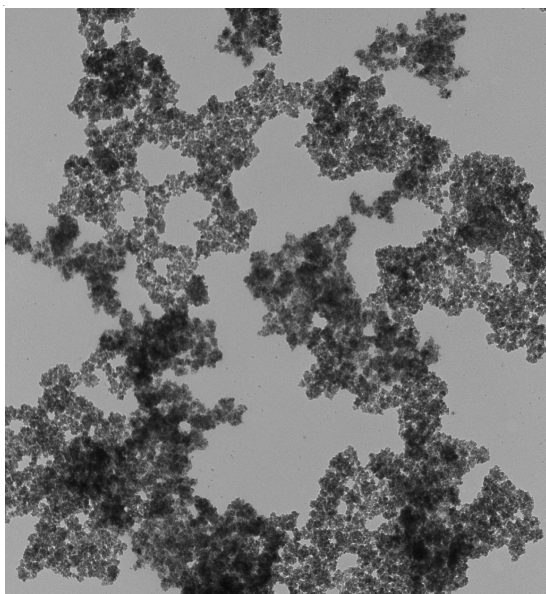


Fig. 4. TEM micrographs for the  $\text{Co}_{0.5}\text{Mn}_{0.5}\text{Fe}_2\text{O}_4$ -chitosan nanoparticles

All of the  $\text{Co}_{0.5}\text{Mn}_{0.5}\text{Fe}_2\text{O}_4$  particles were with uniform distribution. Fig. 4 showed that all the magnetic chitosan particles were below 100 nm.

**SEM:** Figs. 5 and 6 showed the SEM images of the  $\text{Co}_{0.5}\text{Mn}_{0.5}\text{Fe}_2\text{O}_4$  particles and the  $\text{Co}_{0.5}\text{Mn}_{0.5}\text{Fe}_2\text{O}_4$ -chitosan nanoparticles. From the Fig. 5 showed that the  $\text{Co}_{0.5}\text{Mn}_{0.5}\text{Fe}_2\text{O}_4$  particle was about 20 nm and have a spinel crystal structure. Fig. 6 showed the form of the magnetic chitosan nano-particles. The diameter of the magnetic chitosan particles was about 20 nm and the form varied from the spinel structure of the  $\text{Co}_{0.5}\text{Mn}_{0.5}\text{Fe}_2\text{O}_4$  particle to egg-type shape. From Fig. 6, we can see that the surface of magnetic CS particle was tightly wrapped and didn't have  $\text{Co}_{0.5}\text{Mn}_{0.5}\text{Fe}_2\text{O}_4$  particle. It indicated that the  $\text{Co}_{0.5}\text{Mn}_{0.5}\text{Fe}_2\text{O}_4$  particle was wrapped inside the chitosan successfully.

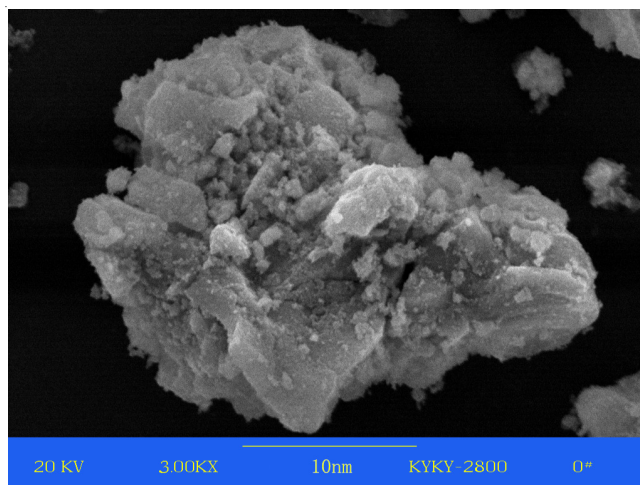


Fig. 5. SEM micrographs for the  $\text{Co}_{0.5}\text{Mn}_{0.5}\text{Fe}_2\text{O}_4$  particles

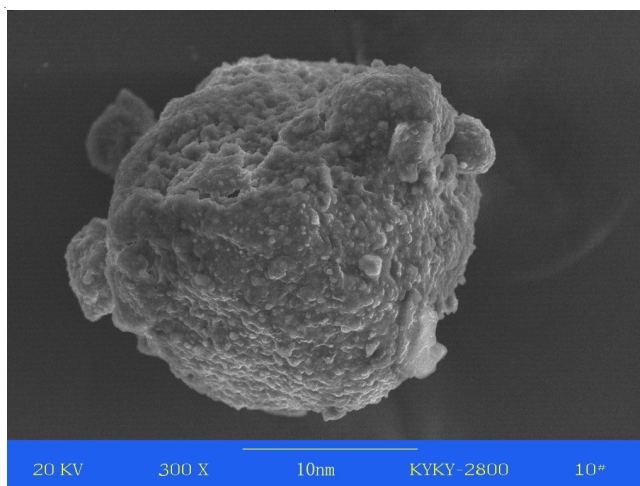


Fig. 6. SEM micrographs for the  $\text{Co}_{0.5}\text{Mn}_{0.5}\text{Fe}_2\text{O}_4$ -chitosan nanoparticles

**Elemental analysis:** The data of elemental analysis in the Table-1 show that the Co, Mn, Fe, in the magnetic composite nanoparticles. The atoms ratio of Fe, Co, Mn was about 4: 1: 1 and it indicated that  $\text{Co}_{0.5}\text{Mn}_{0.5}\text{Fe}_2\text{O}_4$  magnetic particles were encapsulated by chitosan particles integrally.

**Magnetization test:** For magnetic nanoparticles, one of the distinct behaviors is the occurrence of super-paramagnetism which arises from thermal energy overcoming the magnetic

TABLE-1  
ELEMENTAL ANALYSIS OF THE  
MAGNETIC CHITOSAN PARTICLES

Element	C (%)	O (%)	N (%)	Co (%)	Mn (%)	Fe (%)
Content	54.27	28.41	2.23	2.59	2.58	9.82

anisotropy energy barriers of single domain particles. The difference between ferromagnetism and super-paramagnetism is the particle size. The magnetic of particle will change from multi-magnetic domain to mono-magnetic domain and its coercive force enhances with decrease of the scale of particles when the magnetic material is in nano-scale. When the diameter of particles is less than 30 nm, the particles show the character of super-paramagnetism<sup>24</sup>.

In Fig. 7, the magnetic properties of pure  $\text{Co}_{0.5}\text{Mn}_{0.5}\text{Fe}_2\text{O}_4$  particles and magnetic  $\text{Co}_{0.5}\text{Mn}_{0.5}\text{Fe}_2\text{O}_4$ -chitosan nanoparticles were measured. The magnetization of the pure  $\text{Co}_{0.5}\text{Mn}_{0.5}\text{Fe}_2\text{O}_4$  particles was higher than that of the magnetic  $\text{Co}_{0.5}\text{Mn}_{0.5}\text{Fe}_2\text{O}_4$ -chitosan nanoparticles. The magnetization of the pure  $\text{Co}_{0.5}\text{Mn}_{0.5}\text{Fe}_2\text{O}_4$  particles was high as 130 emu/g and that of the magnetic  $\text{Co}_{0.5}\text{Mn}_{0.5}\text{Fe}_2\text{O}_4$ -chitosan nanoparticles was 80 emu/g, meanwhile both of the two particles showed the characteristics of superparamagnetism.

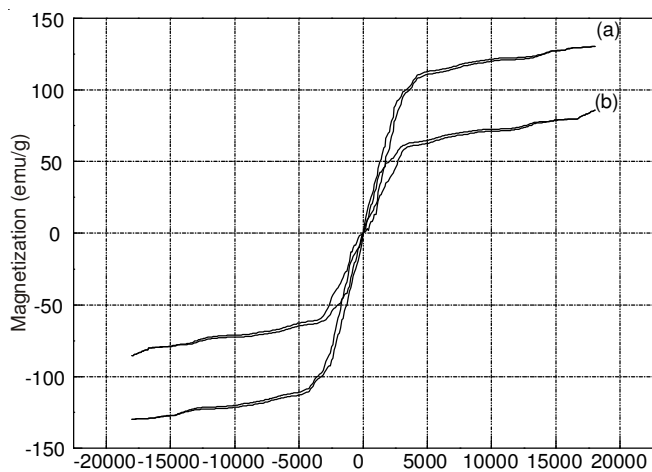


Fig. 7. Field dependence of magnetization for the  $\text{Co}_{0.5}\text{Mn}_{0.5}\text{Fe}_2\text{O}_4$ -chitosan nanoparticles (b) and  $\text{Co}_{0.5}\text{Mn}_{0.5}\text{Fe}_2\text{O}_4$  nanoparticles (a)

**Determination of surface-active:** The density of the crude oil in GD-3, GD-4, GD-6, GD-7 oil block from Shengli Oilfield were 0.97, 0.97, 0.89 and 0.91 g/mL. The main properties of the injected water for each block are shown in Table-2.

TABLE-2  
ION CONCENTRATION AND THE TOTAL  
MINERALIZATION OF THE WATER INTO GD OIL BLOCK

Oil block	Ion concentration (mg/L)					Total mineralization
	$\text{Na}^+$	$\text{Ca}^{2+}$	$\text{Mg}^{2+}$	$\text{Cl}^-$	$\text{HCO}_3^-$	
GD-3	2995.8	207.2	125.9	4831	1437.8	9657.7
GD-4	5164.2	320.8	156.8	10564	480.0	16685.8
GD-6	9507.2	378.3	210	11186.2	599.1	21980.8
GD-7	7414.1	213.2	268.3	8757.7	819.4	17472.7

**Determination of surface-active:** We used the TX-500C full-scale automatic dynamic spinning drop interfacial tension instrument to determine the interfacial activity of the products

on each oil block. When the measurement time was 1 h, the results were shown in Fig. 8. Apparent from the Fig. 8, the  $\text{Co}_{0.5}\text{Mn}_{0.5}\text{Fe}_2\text{O}_4$ -chitosan nanoparticles reduced the oil-water interfacial tension to less than  $10^{-3}$  mN/m in each oil block without any additives. In particular, the products created minimum oil-water interfacial tension to  $5.3 \times 10^{-4}$  mN/m in GD-3 and GD-4 with similar nature. The time to reach a stable oil-water interface tension was short and it can reach the ideal interfacial tension value in 5 min generally. We can see from the Fig. 9 the oil-water interfacial tension were stable. It indicated the products could form a stable flooding system with oil droplets.

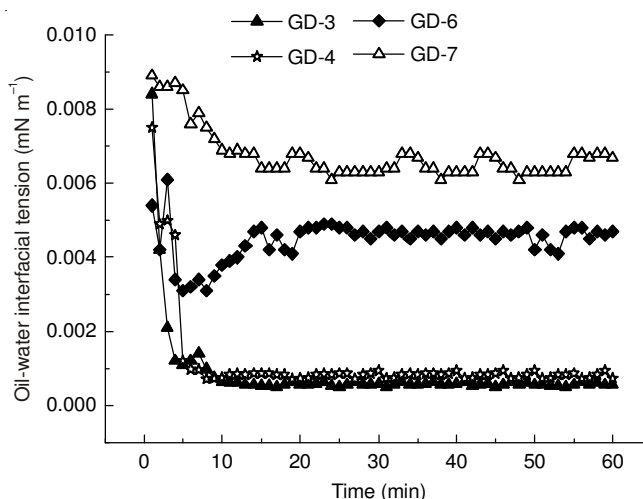


Fig. 8. Dynamic interfacial tension of GD oil block

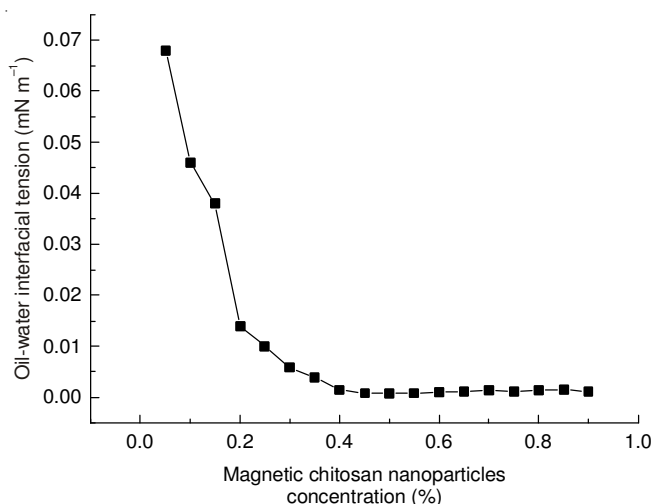


Fig. 9. Effects of  $\text{Co}_{0.5}\text{Mn}_{0.5}\text{Fe}_2\text{O}_4$ -chitosan nanoparticles contents on the interfacial tension

**Product concentration influence on oil-water interfacial tension:** The impact of the  $\text{Co}_{0.5}\text{Mn}_{0.5}\text{Fe}_2\text{O}_4$ -chitosan nanoparticles concentration to oil-water interfacial tension is shown in Fig. 9. Apparent from the Fig. 9, the percentage of products quality was 0.4 % for its CMC point. When percentage of the products was above 0.2 %, the oil-water interfacial tension can reach  $10^{-3}$  mN/m. But a large number of micelles were formed in the solution when the products mass fraction is higher than 0.4 %. So continued to add products on the basis of the percentage of magnetic chitosan nanoparticles quality had little meaning.

**Salt-resisting capacity:** Because salinity of the injected water from different oil blocks varied widely and it affected the oil-water interfacial tension directly, the  $\text{Co}_{0.5}\text{Mn}_{0.5}\text{Fe}_2\text{O}_4$ -chitosan nanoparticles must have good salt-resisting capacity. From the Fig. 10, we can see that the products could reduce oil-water interfacial tension to  $10^{-3}$  mN/m or less when the NaCl concentration was 2500-20000 mg/L. From that, we know the products had good salt-resisting capacity.

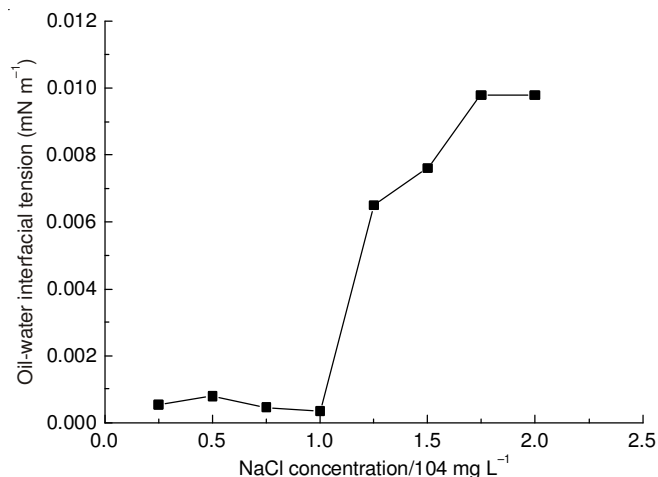


Fig. 10. Effect of sodium ions to interfacial tension

## Conclusion

A novel  $\text{Co}_{0.5}\text{Mn}_{0.5}\text{Fe}_2\text{O}_4$ -chitosan nanoparticles was composed with excellent core/shell structure and magnetic responsive properties. These super-paramagnetic  $\text{Co}_{0.5}\text{Mn}_{0.5}\text{Fe}_2\text{O}_4$ -chitosan nanoparticles were able to reduce surface and interfacial tension to  $10^{-3}$  mN/m and below without any other additives. The time to reach a stable oil-water interface tension was short and it can reach the ideal interfacial tension value in 5 min generally. At the same time, the  $\text{Co}_{0.5}\text{Mn}_{0.5}\text{Fe}_2\text{O}_4$ -chitosan nanoparticles had good salt-resisting capacity.

## ACKNOWLEDGEMENTS

This work was supported by Hebei Education Department Project (Q2012056) and Qinhuangdao Science and Technology Bureau Project (2012021A127).

## REFERENCES

1. S. Mukherjee, P. Das and R. Sen, *Trends Biotechnol.*, **24**, 509 (2006).
2. Y. Wu, J. Guo, W.L. Yang, C.C. Wang and S.K. Fu, *Polymer*, **47**, 5287 (2006).
3. H.W. Gu, K.M. Xu, C.J. Xu and B. Xu, *Chem. Commun.*, **9**, 941 (2006).
4. P. Wunderbaldinger, L. Josephson and R. Weissleder, *Bioconjug. Chem.*, **13**, 264 (2002).
5. W. Wang, L. Deng, Z.H. Peng and X. Xiao, *Enzyme Microb. Technol.*, **40**, 255 (2007).
6. E. Carrero, N.V. Queipo, S. Pintos and L.E. Zerpa, *J. Petrol. Sci. Eng.*, **58**, 30 (2007).
7. M. Nitschke, S.G.V.A.O. Costa and J. Contiero, *Biotechnol. Prog.*, **21**, 1593 (2005).
8. J.D. Van Hamme, A. Singh and O.P. Ward, *Biotechnol. Adv.*, **24**, 604 (2006).
9. R.S. Makkar, S.S. Cameotra and I.M. Banat, *AMB Express*, **1**, 5 (2011).
10. H.-P. Meyer, *Org. Process Res. Dev.*, **15**, 180 (2011).
11. S.L. Fox and G.A. Bala, *Bioresour. Technol.*, **75**, 235 (2000).
12. L.R. Rodrigues, J.A. Teixeira and R. Oliveira, *Biochem. Eng. J.*, **32**, 135 (2006).
13. J. Roger, J.N. Pons, R. Massart, A. Halbreich and J. Bacri, *Eur. Phys. J. Appl. Phys.*, **5**, 321 (1999).
14. I.M. Banat, R.S. Makkar and S.S. Cameotra, *Appl. Microbiol. Biotechnol.*, **53**, 495 (2000).
15. A. Singh, J.D. Van Hamme and O.P. Ward, *Biotechnol. Adv.*, **25**, 99 (2007).
16. J.D. Desai and I.M. Banat, *Microbiol. Mol. Biol. Rev.*, **61**, 47 (1997).
17. W.S.W. Ngah, S. Ab Ghani and A. Kamari, *Bioresour. Technol.*, **96**, 443 (2005).
18. A.J. Varma, S.V. Deshpande and J.F. Kennedy, *Carbohydr. Polym.*, **55**, 77 (2004).
19. Y.C. Chang and D.H. Chen, *J. Colloid Interf. Sci.*, **283**, 446 (2005).
20. C. Shen, H. Chen, S. Wu, Y. Wen, L. Li, Z. Jiang, M. Li and W. Liu, *J. Hazard. Mater.*, **244-245**, 689 (2013).
21. A.C. Zimmermann, A. Mecabo, T. Fagundes and C.A. Rodrigues, *J. Hazard. Mater.*, **179**, 192 (2010).
22. R.B. Hernández, A.P. Franco, O.R. Yola, A. López-Delgado, J. Felcman, M.A.L. Recio and A.L.R. Merce, *J. Mol. Struct.*, **877**, 89 (2008).
23. G. Zhao, J.J. Xu and H.Y. Chen, *Electrochem. Commun.*, **8**, 148 (2006).
24. L. Josephson, Coated with a Polysiloxane and Coupled to a Nucleic Acid, US Patent 4,672,040 (1987).